ResearchGate

See discussions, stats, and author profiles for this publication at: https://www.researchgate.net/publication/10740050

Measurement of Multiple ψ Torsion Angles in Uniformly 13 C, 15 N-Labeled α-Spectrin SH3 Domain Using 3D 15 N– 13 C– 13 C– 15 N MAS Dipolar-Chemical Shift Correlation Spectroscopy

ARTICLE *in* JOURNAL OF THE AMERICAN CHEMICAL SOCIETY · JUNE 2003

Impact Factor: 12.11 · DOI: 10.1021/ja029082c · Source: PubMed

CITATIONS
49

READS
18

5 AUTHORS, INCLUDING:

Vladimir Ladizhansky
University of Guelph
61 PUBLICATIONS **1,592** CITATIONS
SEE PROFILE

Christopher P Jaroniec
The Ohio State University
68 PUBLICATIONS **3,371** CITATIONS
SEE PROFILE

Hartmut Oschkinat
Leibniz-Institut für Molekulare Pharmakologie
171 PUBLICATIONS **6,723** CITATIONS
SEE PROFILE

Robert G Griffin
Massachusetts Institute of Technology
454 PUBLICATIONS **24,502** CITATIONS
SEE PROFILE

Available from: Christopher P Jaroniec
Retrieved on: 15 January 2016

J|A|C|S
ARTICLES
Published on Web 05/09/2003

Measurement of Multiple ψ Torsion Angles in Uniformly $^{13}C,^{15}N$-Labeled α-Spectrin SH3 Domain Using 3D $^{15}N-^{13}C-^{13}C-^{15}N$ MAS Dipolar-Chemical Shift Correlation Spectroscopy

Vladimir Ladizhansky,[†] Christopher P. Jaroniec,[†] Annette Diehl,[‡] Hartmut Oschkinat,[‡] and Robert G. Griffin*,[†]

Contribution from the Department of Chemistry and Center for Magnetic Resonance, Francis Bitter Magnet Laboratory, Massachusetts Institute of Technology, Cambridge, Massachusetts 02139-4307, and Forschungsinstitut für Molekulare Pharmakologie, Robert-Rössle-Strasse 10, 13125 Berlin, Germany

Received October 24, 2002; E-mail: rgg@mit.edu

Abstract: We demonstrate the simultaneous measurement of several backbone torsion angles ψ in the uniformly $^{13}C,^{15}N$-labeled α-Spectrin SH3 domain using two different 3D $^{15}N-^{13}C-^{13}C-^{15}N$ dipolar-chemical shift magic-angle spinning (MAS) NMR experiments. The first NCCN experiment utilizes double quantum (DQ) spectroscopy combined with the INADEQUATE type $^{13}C-^{13}C$ chemical shift correlation. The decay of the DQ coherences formed between $^{13}C'_i$ and $^{13}C_{\alpha i}$ spin pairs is determined by the "correlated" dipolar field due to $^{15}N_i-^{13}C_{\alpha i}$ and $^{13}C'_i-^{15}N_{i+1}$ dipolar couplings and is particularly sensitive to variations of the torsion angle in the regime $|\psi| > 140°$. However, the ability of this experiment to constrain multiple ψ-torsion angles is limited by the resolution of the $^{13}C_\alpha-^{13}CO$ correlation spectrum. This problem is partially addressed in the second approach described here, which is an NCOCA NCCN experiment. In this case the resolution is enhanced by the superior spectral dispersion of the ^{15}N resonances present in the $^{15}N_{i+1}-^{13}C_{\alpha i}$ part of the NCOCA chemical shift correlation spectrum. For the case of the 62-residue α-spectrin SH3 domain, we determined 13 ψ angle constraints with the INADEQUATE NCCN experiment and 22 ψ constraints were measured in the NCOCA NCCN experiment.

Introduction

Over the past decade solid-state NMR (ssNMR) has emerged as an important tool for structural investigations in a variety of biological systems such as membrane and amyloid proteins.[1,2] To date the primary focus of ssNMR experiments has been on systems with isotopic labeling of specific sites.[3−11] Generally, a $^{13}C-^{13}C$ or a $^{13}C-^{15}N$ spin pair is introduced at a specific position in a protein or nucleic acid, and distances[3−8,10] or relative orientations of the anisotropic interactions[9,11] are determined to provide structural constraints. In one of the earliest examples of this approach, the conformation of retinal in the membrane protein bacteriorhodopsin (bR) was determined to be 6-*s-trans* by measuring distances between the 8-^{13}C and 18-^{13}C and 16,17-^{13}C sites.[3,4] More recently, there have been many extensions and applications of this approach.[9−12] In general, the use of $^{13}C-^{13}C$ and $^{13}C-^{15}N$ spin-pair labeling provides precise structural information and will continue to be the method of choice to address a number of specific biological questions.

However, if the experimental goal is a complete structure determination of a biomolecule, then the use of selective labels is inefficient and impractical. In this case large numbers of structural constraints are required,[13] and in recent years approaches based on dipolar recoupling experiments have emerged as ways to achieve spectral assignments and to measure torsion angles and internuclear distances. In particular, recent advances have allowed complete or at least partial assignments in solid, uniformly $^{13}C,^{15}N$-labeled human ubiqutin,[14,15] BPTI,[16] and

[†] Massachusetts Institute of Technology.
[‡] Forschungsinstitut für Molekulare Pharmakologie.

(1) Griffin, R. G. *Nat. Struct. Biol.* **1998**, *5*, 508−512.
(2) Tycko, R. *Annu. Rev. Phys. Chem.* **2001**, *52*, 575−606.
(3) McDermott, A.; Creuzet, F.; Griffin, R. G.; Zawadzke, L. E.; Ye, Q. Z.; Walsh, C. T. *Biochemistry* **1990**, *29*, 5567−5574.
(4) Creuzet, F.; McDermott, A.; Gebhard, R.; van der Hoef, K.; Spijker-Assink, M. B.; Herzfeld, J.; Lugtenburg, J.; Levitt, M. H.; Griffin, R. G. *Science* **1991**, *251*, 783−786.
(5) McDermott, A.; Creuzet, F.; Gebhard, R.; van der Hoef, K.; Levitt, M. H.; Herzfeld, J.; Lugtenburg, J.; Griffin, R. G. *Biochemistry* **1994**, *33*, 6129−6136.
(6) McDowell, L. M.; Klug, C. A.; Beusen, D. D.; Schaefer, J. *Biochemistry* **1996**, *35*, 5395−5403.
(7) McDowell, L. M.; Lee, M.; McKay, A.; Anderson, K. S.; Schaefer, J. *Biochemistry* **1996**, *35*, 3328−3334.
(8) Weliky, D. P.; Bennett, A. E.; Zvi, A.; Anglister, J.; Steinbach, P. J.; Tycko, R. *Nat. Struct. Biol.* **1999**, *6*, 141−145.
(9) Feng, X.; Verdegem, P. J. E.; Eden, M.; Sandstrom, D.; Lee, Y. K.; BoveeGeurts, P. H. M.; Grip, W. J. d.; Lugtenburg, J.; de Groot, H. J. M.; Levitt, M. H. *J. Biomol. NMR* **2000**, *16*, 1−8.
(10) Smith, S. O.; Song, D.; Srinivasan, S.; Groesbeek, M.; ZIliox, M.; Aimoto, S. *Biochemistry* **2001**, *40*, 6553−6558.
(11) Lansing, J. C.; Hohwy, M.; Jaroniec, C. P.; Creemers, A. F. L.; Lugtenburg, J.; Herzfeld, J.; Griffin, R. G. *Biochemistry* **2002**, *41*, 431−438.
(12) Shaw, W. J.; Long, J. R.; Dindot, J. L.; Campbell, A. A.; Stayton, P. S.; Drobny, G. P. *J. Am. Chem. Soc.* **2000**, *122*, 1709−1716.
(13) Wüthrich, K. *NMR of Proteins and Nucleic Acids*; Wiley: New York, 1986.
(14) Straus, S. K.; Bremi, T.; Ernst, R. R. *J. Biomol. NMR* **1998**, *12*, 39−50.
(15) Hong, M. *J. Biomol. NMR* **1999**, *15*, 1−14.

α-spectrin SH3 domain.[17,18] More recently, the backbone structure of α-spectrin SH3 domain has been determined from a large number of distance constraints.[19]

An essential component of structural studies is the measurement of internuclear distances. In multiple-spin systems, however, the structurally important weak dipolar interactions can be obscured by the strong couplings between directly bonded nuclei.[20−23] This problem can be partially overcome by utilizing spectrally selective heteronuclear[24] and homonuclear[25−27] techniques for distance measurements. Alternatively, in certain cases $^{13}C-^{15}N$ distances can be simultaneously measured in uniformly labeled systems using 3D experiments[28,29] based on rotational echo double resonance (REDOR)[30] and transferred echo double resonance (TEDOR)[31,32] techniques.

Another important class of experiments that emerged in recent years, correlates the relative orientation of anisotropic chemical shift or dipolar interactions, or both[33−39] and are used to measure the backbone and side-chain torsion angles ϕ, ψ and χ.[33−39] However, in uniformly labeled solids, the applicability of these methods can be limited by insufficient spectral resolution. This may be a significant complication in larger peptides[40] and proteins[14−17,19] where cross-peaks start to overlap, making interpretation of the experimental data a complicated task. The existing methods for correlating anisotropic interactions should therefore be extended and combined with the chemical shift correlation techniques that provide site-specific resolution to allow simultaneous determination of multiple torsion angle constraints in a single experiment. This approach has been employed previously in the 3D $^{1}H-^{15}N-^{13}C-^{1}H$ torsion angle experiments described elsewhere.[38] The multiple torsion angle constraints determined in these experiments, together with the $^{13}C-^{15}N$ distance constraints obtained by frequency selective REDOR measurements,[24] has led to a complete high-resolution structure of the tripeptide *N*-formyl-Met-Leu-Phe-OH (*N*-f-MLF-OH).[41]

In this publication we demonstrate the feasibility of simultaneously determining the ψ-torsion angles in uniformly labeled proteins. The experiments were conducted on the 62-residue α-spectrin SH3 domain. The experimental schemes investigated here are related, and both are based on the existing $^{15}N-^{13}C-^{13}C-^{15}N$[36,37] torsion angle experiment, which is sensitive to the variation of the absolute value of torsion angle ψ in the vicinity of its trans conformation: $|\psi| > 140°$. The NCCN dipolar correlation method uses the simple fact that the relative orientation of the $N_i-C_{\alpha i}$ and the C'_i-N_{i+1} chemical bonds and therefore the $^{15}N_i-^{13}C_{\alpha i}$ and $^{13}C'_i-^{15}N_{i+1}$ dipolar tensors is a function of the torsion angle ψ_i. In the first, INADEQUATE NCCN experiment[36,37] studied here the correlation of the $^{15}N_i-^{13}C_{\alpha i}$ and $^{13}C'_i-^{15}N_{i+1}$ dipolar tensors is achieved by creating a double quantum (DQ) state between the $^{13}C_{\alpha i}$ and $^{13}C'_i$ spins, and letting it dephase under the $^{15}N_i-^{13}C_{\alpha i}$ and $^{13}C'_i-^{15}N_{i+1}$ dipolar couplings that are simultaneously reintroduced by REDOR. The decay of the DQ coherence as a function of the length of the dipolar evolution is therefore determined by the "correlated" dipolar field due to the $^{15}N_i-^{13}C_{\alpha i}$ and $^{13}C'_i-^{15}N_{i+1}$ dipolar couplings. The dipolar dephasing is followed by the DQ chemical shift evolution period, and the experiment therefore combines the NCCN dipolar correlation method and the DQ-single quantum (DQ-SQ) $^{13}C-^{13}C$ INADEQUATE[42] chemical shift correlation for spectral resolution. Using spectra recorded at 500 MHz, a total of 13 ψ torsion angle constraints were obtained from this experiment. At higher fields where additional spectral resolution is available, additional measurements would be possible.

The novel feature of the second, NCOCA NCCN experiment presented here is that the dipolar evolution is split into two separate periods in which $^{15}N_i-^{13}C_{\alpha i}$ and $^{13}C'_i-^{15}N_{i+1}$ dipolar interactions are recoupled separately, allowing incorporation of the ^{15}N chemical shift evolution period. The advantage of this experiment is based on the superior $^{15}N_{i+1}-^{13}C_{\alpha i}$ spectral resolution of the NCOCA chemical shift correlation spectrum. A total of 22 ψ torsion angle constraints were determined by this method. Again the number of constraints would increase when the experiment is moved to higher fields. To the best of our knowledge, this is the first time that multiple torsion angle constraints have been determined in a uniformly labeled protein.

Experimental Section

Sample Preparation. The preparation of the α-spectrin SH3 domain for NMR experiments is described elsewhere.[17] Approximately 25 mg of the protein was transferred into a thin wall 4-mm Chemagnetics (Fort Collins, CO) rotor. The sample was constrained to the middle part of the rotor by spacers to minimize effects of rf inhomogeneity and sealed to prevent dehydration.

(16) McDermott, A.; T. Polenova, T.; Bockmann, A.; Zilm, K. W.; Paulsen, E. K.; Martin, R. W.; Montelione, G. T. *J. Biomol. NMR* **2000**, *16*, 209−219.
(17) Pauli, J.; Baldus, M.; van Rossum, B.-J.; de Groot, H. J. M.; Oschkinat, H. *ChemBioChem* **2001**, *2*, 272−281.
(18) van Rossum, B.-J.; Castellani, F.; Rehbein, K.; Pauli, J.; Oschkinat, H. *ChemBioChem* **2001**, *2*, 906−914.
(19) Castellani, F.; van Rossum, B.-J.; Diehl, A.; Schubert, M.; Rehbein, K.; Oschkinat, H. *Nature* **2002**, *420*, 98−102.
(20) Costa, P. R. *Spins, Peptides, and Alzheimer's Disease: Solid-State Nuclear Magnetic Resonance Investigations of Amyloid Peptide Conformation*; Massachusetts Institute of Technology: Cambridge, MA, 1996.
(21) Hohwy, M.; Rienstra, C. M.; Jaroniec, C. P.; Griffin, R. G. *J. Chem. Phys.* **1999**, *110*, 7983−7992.
(22) Hodgkinson, P.; Emsley, L. *J. Magn. Reson.* **1999**, *139*, 46−59.
(23) Ladizhansky, V.; Vega, S. *J. Chem. Phys.* **2000**, *112*, 7158−7166.
(24) Jaroniec, C. P.; Tounge, B. A.; Herzfeld, J.; Griffin, R. G. *J. Am. Chem. Soc.* **2001**, 3507−3519.
(25) Raleigh, D. P.; Levitt, M. H.; Griffin, R. G. *Chem. Phys. Lett.* **1988**, *146*, 71−76.
(26) Takegoshi, K.; Nomura, K.; Terao, T. *Chem. Phys. Lett.* **1995**, *232*, 424−428.
(27) Costa, P. R.; Sun, B.; Griffin, R. G. *J. Am. Chem. Soc.* **1997**, *119*, 10821−10836.
(28) Michal, C. A.; Jelinski, L. W. *J. Am. Chem. Soc.* **1997**, *119*, 9059−9060.
(29) Jaroniec, C. P.; Filip, C.; Griffin, R. G. *J. Am. Chem. Soc.* **2002**, *124*, 10728−10742.
(30) Gullion, T.; Schaefer, J. *J. Magn. Reson.* **1989**, *81*, 196−200.
(31) Hing, A. W.; Vega, S.; Schaefer, J. *J. Magn. Reson.* **1992**, *96*, 205−209.
(32) Hing, A. W.; Vega, S.; Schaefer, J. *J. Magn. Reson. A* **1993**, *103*, 151−162.
(33) Feng, X.; Lee, Y. K.; Sandström, D.; Eden, M.; Maisel, H.; Sebald, A.; Levitt, M. H. *Chem. Phys. Lett.* **1996**, *257*, 314−320.
(34) Hong, M.; Gross, J. D.; Griffin, R. G. *J. Phys. Chem. B* **1997**, *101*, 5869−5874.
(35) Hong, M.; Gross, J. D.; Hu, W.; Griffin, R. G. *J. Magn. Reson.* **1998**, *135*, 169−177.
(36) Feng, X.; Eden, M.; Brinkmann, A.; Luthman, H.; Eriksson, L.; Gräslund, A.; Antzutkin, O. N.; Levitt, M. H. *J. Am. Chem. Soc.* **1997**, *119*, 12006−12007.
(37) Costa, P. R.; Gross, J. D.; Hong, M.; Griffin, R. G. *Chem. Phys. Lett.* **1997**, *280*, 95−103.
(38) Rienstra, C. M.; Hohwy, M.; Mueller, L. J.; Jaroniec, C. P.; Reif, B.; Griffin, R. G. *J. Am. Chem. Soc.* **2002**, *124*, 11908−11922.
(39) Ladizhansky, V.; Veshtort, M.; Griffin, R. G. *J. Magn. Reson.* **2002**, *154*, 317−324.
(40) Detken, A.; Hardy, E. H.; Ernst, M.; Kainosho, M.; Kawakami, T.; Aimoto, S.; Meier, B. H. *J. Biomol. NMR* **2001**, *20*, 203−221.
(41) Rienstra, C. M.; Tucker-Kellogg, L.; Jaroniec, C. P.; Hohwy, M.; Reif, B.; McMahon, M. T.; Tidor, B.; Lozano-Perez, T.; Griffin, R. G. *Proc. Natl. Acad. Sci. U.S.A.* **2002**, *99*, 10260−10265.
(42) Hohwy, M.; Rienstra, C. M.; Griffin, R. G. *J. Chem. Phys.* **2002**, *117*, 4973−4987.

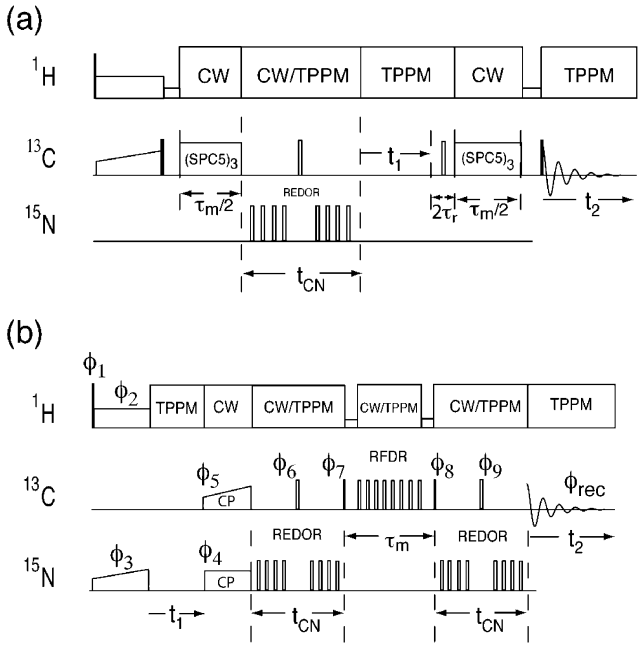

Figure 1. Three-dimensional INADEQUATE-type NCCN (a) and NCOCA NCCN (b) chemical shift dipolar correlation pulse sequences. Solid and open rectangles represent $\pi/2$ and π pulses, respectively. In (a), following ^{1}H to ^{13}C CP, SPC5$_3$ pulse sequence[42] excites DQ coherences between $^{13}C_{\alpha i}$ and $^{13}C'_i$ carbons, which evolve under the $^{13}C_{\alpha i}$–$^{15}N_i$ and $^{13}C'_i$–$^{15}N_{i+1}$ dipolar couplings reintroduced by REDOR. The dipolar evolution period is followed by the DQ chemical shift evolution. The π-pulse at the end of the chemical shift evolution period prepares DQ coherences for reconversion.[33] The DQ coherences are then converted into SQ, and the DQ path is selected by the standard phase cycling.[45] In (b), the ^{1}H to ^{15}N CP creates $^{15}N_{i+1}$ magnetization that evolves under the chemical shifts. The magnetization is transferred selectively to $^{13}C'_i$ carbons and dephased under the $^{13}C'_i$–$^{15}N_{i+1}$ and $^{15}N_{\alpha i}$–$^{13}C_{\alpha i}$ dipolar couplings in two consecutive periods. The phase cycles in (b) were: $\phi_1 = 8 \times 1, 8 \times 3$, $\phi_2 = 2$, $\phi_3 = 4 \times (13)$, $\phi_4 = 1$, $\phi_5 = 11223344$, $\phi_6 = 1$, $\phi_7 = 24314213$, $\phi_8 = 42132431$, $\phi_9 = 1$, $\phi_{rec} = 13243142\ 31421324$, where $1 = x$, $2 = y$, $3 = -x$, $4 = -y$. The ^{15}N REDOR and ^{13}C RFDR pulses were phase-cycled according to XY-4[46] and XY-8[47] schemes, respectively. Hypercomplex data were acquired by shifting ϕ_4 according to Ruben and co-workers.[48] The decoupling during the REDOR and RFDR sequences alternated between CW and TPPM irradiation during pulses and free precession periods, respectively.[24]

NMR Experiments. NMR experiments were performed on a Cambridge Instrument spectrometer (courtesy of Dr. D. J. Ruben) operating at 11.7 T (500.06 MHz for ^{1}H, 125.7 MHz for ^{13}C, and 50.6 MHz for ^{15}N) equipped with a 4-mm triple resonance Chemagnetics (Fort Collins, CO) probe. The MAS rate was 9.523 kHz in all experiments and controlled by Doty Scientific (Columbia, SC) spinning frequency controller with a stability of ± 3 Hz. The experiments were conducted at $\sim$0 °C to prevent sample heating due to high decoupling powers.

The INADEQUATE-type[21] NCCN experiment is illustrated in Figure 1a. Here, the excitation of the DQ coherences between $^{13}C_{\alpha i}$ and $^{13}C'_i$ spins is followed by the dipolar evolution period where the DQ coherences evolve under the $^{13}C_{\alpha i}$–$^{15}N_i$ and $^{13}C'_i$–$^{15}N_{i+1}$ couplings reintroduced by REDOR sequence. The DQ coherences evolve under their chemical shifts, defining the t_1 chemical shift dimension of the experiment. This period is followed by a conversion of the DQ to a SQ for detection. The dipolar dephasing of a cross-peak as a function of the dipolar evolution time t_{CN} depends on the relative orientation of the $^{15}N_i$–$^{13}C_{\alpha i}$ and $^{13}C'_i$–$^{15}N_{i+1}$ dipolar tensors, and therefore on the torsion angle ψ_i. The NCOCA NCCN experiment shown in Figure 1b employs the same principle of correlating $^{15}N_i$–$^{13}C_{\alpha i}$ and $^{13}C'_i$–$^{15}N_{i+1}$ dipolar couplings. Following the ^{1}H–^{15}N cross polarization (CP)[43] the coherence transfer pathway is:

$$N_{x,i+1} \xrightarrow{t_1} N_{x,i+1}\exp(i\omega_{N_{i+1}}t_1) \xrightarrow{\text{DCP}} C'_{ix}\exp(i\omega_{N_{i+1}}t_1) \xrightarrow{t_{CN}}$$
$$C'_{ix}c_1\exp(i\omega_{N_{i+1}}t_1) \xrightarrow{\text{RFDR}} C_{\alpha ix}c_1\exp(i\omega_{N_{i+1}}t_1) \xrightarrow{t_{CN}}$$
$$C_{\alpha ix}c_1c_2\exp(i\omega_{N_{i+1}}t_1) \xrightarrow{t_2} C_{\alpha ix}c_1c_2\exp(i\omega_{N_{i+1}}t_1)\exp(i\omega_{C_{ai}}t_2)$$

To simplify the notation, we assume that the RFDR polarization transfer period includes also $\pi/2$ flip-up preparation and flip-down read out pulses (see Figure 1b). We also assume quadrature detection in the indirect t_1 and direct t_2 dimensions of the experiment.

Here, the symbols N_{ix} and C_{ix} denote $^{15}N_i$ and $^{13}C_i$ spin operators, respectively, and $c_1 = \cos(\omega_d^{C'_iN_{i+1}}t_{CN})$, $c_2 = \cos(\omega_d^{C_{\alpha i}N_i}t_{CN})$. The transverse $N_{x,i+1}$ magnetization evolves under the chemical shift for frequency labeling. The band-selective CP[44] creates transverse magnetization on carbonyl carbons. Subsequently, a REDOR period initiated for a time t_{CN}, reintroduces ^{13}C–^{15}N dipolar couplings, and the transverse magnetization of carbonyl $^{13}C'_i$ carbons will acquire modulation that is dominated by the strongest $^{13}C'_i$–$^{15}N_{i+1}$ couplings with directly bonded $^{15}N_{i+1}$. The RFDR period transfers polarization from $^{13}C'_i$ spins to the directly bonded $^{13}C_{\alpha i}$ spins. The second REDOR period, initiated for the same time t_{CN} as the first one, reintroduces $^{13}C_{\alpha i}$–$^{15}N_i$ couplings.

The $^{13}C_{\alpha i}$ magnetization is detected during acquisition in t_2. After 2D Fourier transformation, the intensities of the cross-peaks for each crystallite, occurring at the frequencies $(\omega_{N_{i+1}},\omega_{C_{\alpha i}})$ in the NCOCA ^{15}N–^{13}C correlation spectrum will be modulated as a function of the dipolar evolution time t_{CN}, as $\cos(\omega_d^{C'_iN_{i+1}}t_{CN})\cos(\omega_d^{C_{\alpha i}N_i}t_{CN})$, therefore resulting in the dependence identical to that in the INADEQUATE NCCN experiment.[36,37] However, the $^{15}N_{i+1}$–$^{13}C_i$ resolution in the NCOCA experiment is expected to be better.

Another factor contributing to the intensity decay of the cross-peaks is transverse relaxation during dipolar evolution. A reference experiment without π-pulses on the ^{15}N channel is performed to correct for these effects, as in conventional REDOR. The dephasing of the cross-peaks in the reference experiment is then determined by T_2. In the following discussion, the decay curve resulting from the reference experiment will be denoted S_0, and for the experiment with the REDOR π-pulses, S.

The SPC5$_3$ pulse sequence[42] was used to generate DQ coherences in the INADEQUATE NCCN experiment using a ^{13}C $\omega_1/2\pi = 31.7$ kHz. A DQ excitation efficiency of 30–35% was achieved. The band selective $^{15}N_{i+1}$ to $^{13}C'_i$ CP[44] was used in the NCOCA NCCN experiment. To avoid possible interference between the ^{15}N rf field and the ^{1}H decoupling field during REDOR, relatively long π-pulses of 16 μs were used on the ^{15}N channel, and CW proton decoupling rf field was $\sim$110 kHz during the pulses and TPPM decoupling[49] of $\sim$100 kHz during free precession periods.

The radio-frequency driven recoupling (RFDR)[47] sequence with an XY-8 phase cycling scheme was used for $^{13}C'_i$ to $^{13}C_{\alpha i}$ polarization transfer. The length of the carbon π-pulse was 10 μs. TPPM decoupling of $\sim$86 kHz was employed between the pulses, and a CW field of $\sim$100 kHz was used during RFDR pulses. A ^{1}H rf field of 75 kHz was used for TPPM decoupling during acquisition, with total phase shift $\phi = 12°$.

Determination of the Torsion Angle ψ. Simulations. Experimental results were analyzed using the expression

(43) Pines, A.; Gibby, M. G.; Waugh, J. S. *J. Chem. Phys.* **1973**, *59*, 569–590.
(44) Baldus, M.; Petkova, A. T.; Herzfeld, J.; Griffin, R. G. *Mol. Phys.* **1998**, *95*, 1197–1207.
(45) Ernst, R. R.; Bodenhausen, G.; Wokaun, A. *Principles of Nuclear Magnetic Resonance in One and Two Dimensions*; Clarendon Press; Oxford, 1991.
(46) Gullion, T.; Baker, D. B.; Conradi, M. S. *J. Magn. Reson.* **1990**, *89*, 479–484.
(47) Bennett, A. E.; Rienstra, C. M.; Griffiths, J. M.; Zhen, W.; Lansbury, P. T.; Griffin, R. G. *J. Chem. Phys.* **1998**, *108*, 9463–9479.
(48) States, D. J.; Haberkorn, R. A.; Ruben, D. J. *J. Magn. Reson.* **1982**, *48*, 286–292.
(49) Bennett, A. E.; Rienstra, C. M.; Auger, M.; Lakshmi, K. V.; Griffin, R. G. *J. Chem. Phys.* **1995**, *103*, 6951–6957.

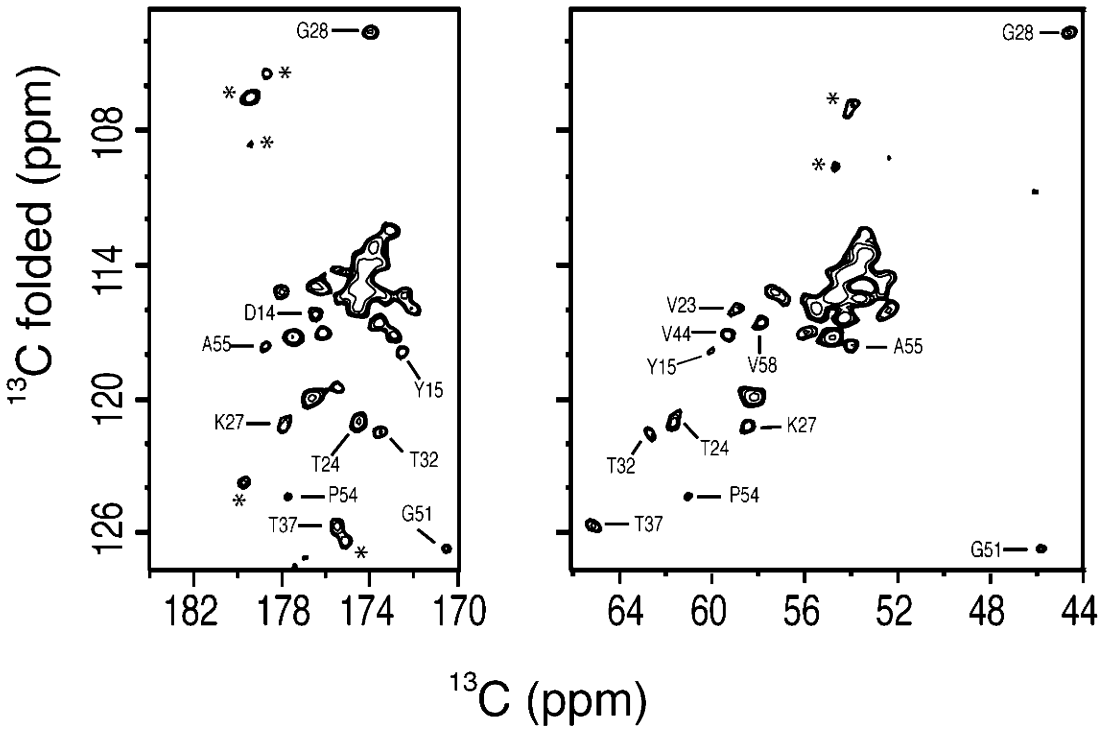

Figure 2. The DQ-SQ $^{13}C-^{13}C$ correlation spectrum of the α-spectrin SH3 domain obtained with the pulse sequence of Figure 1a with $t_{CN} = 0$. The $C_{\alpha i}-C'_i$ correlations are assigned according to the corresponding residues. In the CO part of the spectrum on the left, the asterisks indicate correlations involving carboxylic carbons from Asp, Asn, Glu, Gln residues. In the C_α part of the spectrum on the right, the asterisks indicate cross-peaks due to formation of DQ coherences between $^{13}C_{\alpha i}$ and $^{13}C_{\beta i}$. The spectral assignments of $^{13}C_{\alpha i}$ and $^{13}C_{\beta i}$ resonances were known a priori and the corresponding DQ-SQ correlation spectrum was precalculated to avoid any overlap between the $^{13}C_{\alpha i}-^{13}C_{\beta i}$ and $C_{\alpha i}-C'_i$ cross-peaks. The position of the carrier frequency was 115 ppm, approximately in the middle between CO and CA resonances. Thirty-two points were taken in the t_1 dimension with the increment of 315 μs. Eight points were taken in the dipolar dimension. For *S* curve, the numbers of scans for each FID varied with t_{CN} and were 96, 192, 256, 512, 512, 512, 512, 512 for $t_{CN} = 2\tau_r \times (0,2,3,4,5,6,7,8)$, respectively. The number of scans in the reference experiment was kept 96 for all t_{CN} values. Prior to taking S/S_0 ratio, the cross-peak intensities extracted from the *S* and S_0 experiments were normalized per number of scans.

$$\frac{S}{S_0} = \langle f(\tau_m)\cos(\omega_d^{C_\alpha N_i} t_{CN})\cos(\omega_d^{C'N_{i+1}} t_{CN}) \times \cos(\omega_d^{C_\alpha N_{i+1}} t_{CN})\cos(\omega_d^{C'N_i} t_{CN})\rangle_\Omega \quad (1)$$

where $f(\tau_m) = \sin^2(\omega_d^{CC}\tau_m)$ is the SPC5$_3$ or RFDR polarization transfer function for INADEQUATE or NCOCA NCCN experiments, respectively. The $\langle f(\tau_m).....\rangle_\Omega$ indicates a powder average. The dephasing of the signal described by eq 1 is mainly determined by the strength of the two dipolar couplings $\omega_d^{C_\alpha N_i}$ and $\omega_d^{C'_i N_{i+1}}$ in the directly bonded $^{13}C-^{15}N$ spin pairs. The weaker two-bond couplings $\omega_d^{C_{\alpha i} N_{i+1}}$, $\omega_d^{C'_i N_i}$, and the anisotropic character of the polarization transfer function $f(t_m)$ have a minor effect on the dephasing.[37] However, their orientations are uniquely determined by ψ and hence they can be easily incorporated into the expression for the signal decay. The effective heteronuclear dipolar coupling $\omega_d{}^{AB}$ between two nuclei A, B (A = $^{13}C'_i$, $^{13}C_{\alpha i}$, B = $^{15}N_i$,$^{15}N_{i+1}$) depends on the crystal orientation and can be written as:[50,51]

$$\omega_d{}^{AB} = -\frac{4}{\pi} k\{\mathrm{Im}\}(\omega_{(1)}{}^{AB})$$
$$\omega_{(1)}{}^{AB} = \frac{\mu_0}{4\pi}\frac{\gamma_A\gamma_B}{r_{AB}{}^3}\sum_{m=-2}^{m=2} D^{(2)}_{0,m}(\Omega^{AB}_{PM}) D^{(2)}_{m,-1}(\Omega) d^{(2)}_{-1,0}(\theta_m) \quad (2)$$

The Wigner rotation matrix $D^{(2)}_{0,m}(\Omega^{AB}_{PM})$ describes the transformation of the corresponding AB dipolar tensor from its principal axis system (PAS) to the molecular frame with its axis *z* along the $C'_i-C_{\alpha i}$ bond. The Euler angles Ω are random variables in a powder and relate the molecular frame to a rotor frame. The element $d^{(2)}_{-1,0}(\theta_m)$ of the reduced rotation matrix corresponds to the transformation of the rotor-fixed frame into the laboratory frame via a rotation by the magic angle $\theta_m = 54.7°$. The PAS for the $^{13}C'_i-^{13}C_{\alpha i}$ tensor coincides with the molecular frame, and the corresponding expressions for the effective dipolar constant ω_d^{CC} for SPC5$_3$ and RFDR sequences can be found elsewhere.[42,47] The scaling factor *k* is determined by the REDOR finite pulse effects[52] and vibrational effects[53] and can be estimated experi-

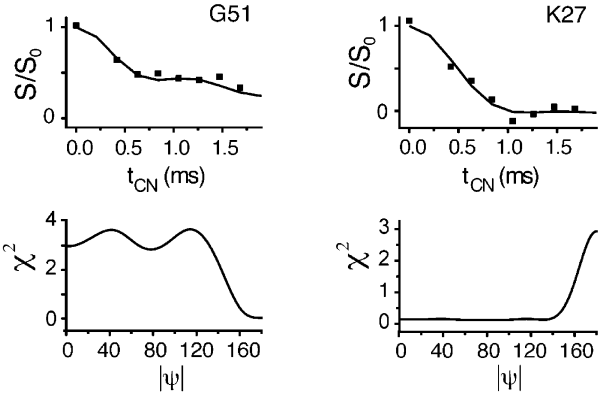

Figure 3. Two representative dipolar dephasing curves obtained from the INADEQUATE NCCN experiment with the best fits and the corresponding χ_ν^2 curves.

(50) Bennett, A. E.; Griffin, R. G.; Vega, S. Recoupling of Homo- and Heteronuclear Dipolar Interactions in Rotating Solids. In *Solid State NMR IV: Methods and Applications of Solid-State NMR*; Blumich, B., Ed.; Springer-Verlag: Berlin, 1994; pp 1−77.
(51) Mehring, M. *Principles of High-Resolution NMR in Solids*; Springer-Verlag: Berlin, 1983.

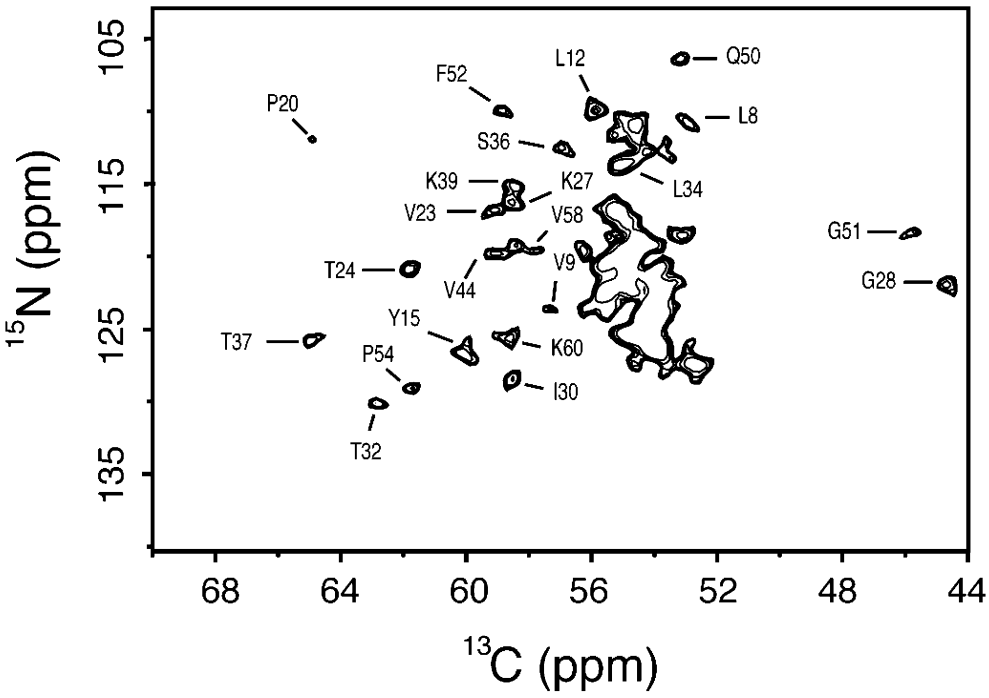

Figure 4. Spectrum at 500 MHz illustrating the $^{13}C_{\alpha i}-^{15}N_{i+1}$ region from the NCOCA NCCN experiment obtained with the sequence of Figure 1b with $t_{CN} = 0$. The cross-peaks are labeled according to their $C_{\alpha i}$ assignments. Thirty-two points were taken in the t_1 dimension with the increment of 315 μs. Seven points were taken in the dipolar dimension. For *S*-curve, the numbers of scans for each FID varied with t_{CN} and were 256, 256, 512, 640, 640, 1024, 1024 for $t_{CN} = 2\tau_r \times (0,2,3,4,5,6,7)$, respectively. The number of scans in the reference experiment was kept at 256 for all t_{CN} values. Prior to taking S/S_0 ratio, the cross-peak intensities extracted from the *S* and S_0 experiments were divided per number of scans.

mentally from the dephasing of the $^{13}C_{\alpha i}-^{13}C_{\beta i}$ cross-peaks denoted by asterisks in the C_α region of the INADEQUATE spectrum of Figure 2. The decay of these peaks as a function of the dipolar evolution time is mainly determined by the strong $^{13}C_{\alpha i}-^{15}N_i$ dipolar couplings and should therefore exhibit a typical REDOR-type behavior. In practice, the REDOR decay of the resolved $^{13}C_{\alpha i}-^{13}C_{\beta i}$ cross-peaks was measured and the effective dipolar couplings were extracted and used in the simulations. The standard backbone geometry used in the simulations was as follows: C'_i-C_α bond, 1.52 Å; C'_i-N_{i+1}, 1.33 Å; $C_{\alpha i}-N_i$ bond, 1.45 Å; $N_i-C_{\alpha i}-C'_i$ bond angle, 110.7°; $C_{\alpha i}-C'_i-N_{i+1}$ bond angle, 115.6°. The effective dipolar couplings were found to be scaled by 0.95 compared to this model.

Error Analysis. The best fit to the ψ torsion angle was determined by minimizing the χ_ν^2 function

$$\chi_\nu^2 = \frac{1}{n-1}\sum_i \left(\frac{S_i - E_i}{\sigma_i}\right)^2 \qquad (3)$$

where E_i is the experimental value for data point, S_i is the simulated value for data point, and the dispersions σ_i's were estimated from the experimental noise. The dihedral angle ψ was the only free parameter in the fitting simulation. Error limits for the torsion angles were determined using an *F*-test at the 90% confidence level.[54] The possible systematic errors due to deviations in the bond angles and $^{13}C-^{15}N$ distances from the standard backbone parameters were discussed elsewhere.[37]

These errors are much smaller than the experimentally observed random errors, and can therefore be neglected. Only the absolute value of the torsion angle can be determined from these experiments.

Experimental Results

The spectral assignments were confirmed using the dipolar INADEQUATE[21] DQ-SQ $^{13}C-^{13}C$ correlation spectrum shown in Figure 2 and the NCOCA chemical shift correlation spectrum illustrated in Figure 4. The isotropic chemical shifts determined from these spectra were within 0.1 ppm of the reported shifts.[17] There are 10 and 12 well-resolved cross-peaks in the CO and CA regions, respectively. Among 10 cross-peaks of interest resolved in the CO region of the spectrum in Figure 2, the D14, T24, and G51 residues show relatively slow decays, indicative of the torsion angle ψ being in the range $|\psi| = 140-180°$.[36,37] For example, the dephasing of the G51 cross-peak shown in Figure 3, agrees well with the $|\psi|$ conformation of 180°, as evident from the corresponding χ_ν^2 plot. In contrast, the cross-peak intensities corresponding to Y15, K27, G28, T32, T37, P54, A55 residues decay fast, and the corresponding values for $|\psi|$ were found to be in the insensitive region of the NCCN experiment, $|\psi| < 140°$. Figure 3 illustrates the dephasing curve for the K27 residue. As can be clearly seen from the corresponding χ_ν^2 curve, all $|\psi|$ values below <140° can occur with nearly equal probability. Most of the peaks resolved in the CO region are fully resolved in the C_α region as well. However, a few extra peaks appear in the C_α part of the spectrum. For example, the cross-peaks between the $^{13}C'_i$ and $^{13}C_{\alpha i}$ carbons in V23, V44, and V58 residues are clearly seen. These three residues dephase slowly, indicating that the corresponding $N_iC_{\alpha i}C'_iN_{i+1}$ dihedral angles are close to $|\psi| = 180°$. The values of the torsion angles ψ, measured in the INADEQUATE NCCN experiment are summarized in Table 1.

An alternative experimental scheme, which provides improved spectral resolution, is based on the NCOCA chemical shift

(52) Jaroniec, C. P.; Tounge, B. A.; M., R. C.; Herzfeld, J.; Griffin, R. G. *J. Magn. Reson.* **2000**, *146*, 132−139.
(53) Ishii, Y.; Terao, T.; Hayashi, S. *J. Chem. Phys.* **1997**, *107*, 2760−2774.
(54) Shoemaker, D. P.; Garland, C. W.; Nibler, J. W. *Experiments in Physical Chemistry*; McGraw-Hill: New York, 1989.

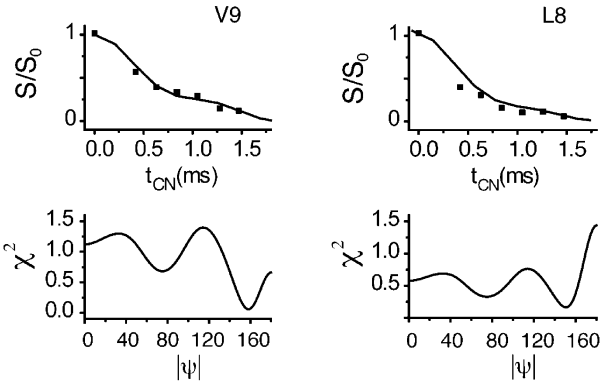

Figure 5. Two representative dipolar dephasing curves obtained from the NCOCA NCCN experiment with the best fits and the corresponding χ_ν^2 curves.

correlation and shown in Figure 1b. In this case the dipolar evolution period is split into two separate periods in which $^{13}C'_i-^{15}N_{i+1}$ and $^{15}N_i-^{13}C_{\alpha i}$ dipolar interactions are recovered, respectively. The $^{15}N_{i+1}-^{13}C_{i\alpha}$ region of the NCOCA correlation spectrum shown in Figure 4 has better resolution than the INADEQUATE NCCN spectrum, and there are 22 resolved cross-peaks in the spectrum.

In this case the cross-peaks due to V9, V23, T24, V44, G51, and V58 residues decay slower than the other cross-peaks, indicating that $|\psi| = 140-180°$. An example of the dephasing of the V9 cross-peak as a function of the dipolar evolution t_{CN} is shown in Figure 5. The corresponding χ_ν^2 plot has one deep minimum corresponding to the absolute value for the torsion angle of 158°.

The L8, Q50, and F52 residues dephase more rapidly and have two minima of comparable depth in the χ_ν^2 plot, as shown in Figure 5, indicating that the experimental data can be fit to a family of conformations centered around these minima.

The rest of the curves are in the insensitive region of the experiment,. and one can only conclude that the absolute value of the torsion angle in these residues is smaller than approximately 145°. The values for the torsion angles determined at the 90% confidence level are listed in the Table 1. Two experimental schemes discussed above should lead to similar dephasing curves. A few considerations should be taken into account when deciding what experiment to choose. The INADEQUATE NCCN experiment has a few important advantages over the NCOCA NCCN scheme. First, the initial signal loss in the INADEQUATE experiment is defined by the efficiency of the double quantum filter, which is on the order of 30−35%. In comparison, the NCOCA experiment involves two polarization transfer steps: $^{15}N_{i+1}$ to $^{13}C'_i$ CP, and $^{13}C'_i$ to $^{13}C_{\alpha i}$ RFDR transfer, with overall efficiency of approximately 20%.

Second, while in the DQ state, the *J*-couplings do not affect the dipolar evolution of the DQ coherences in the INADEQUATE experiment. The decay of the DQ coherences will therefore be determined by the $^{13}C-^{15}N$ dipolar couplings as well as by the transverse relaxation. In contrast, the *J*-couplings are active during the REDOR dipolar evolution in the NCOCA NCCN experiment, which results in additional signal reduction and will therefore require more averaging to achieve the same signal-to-noise as that in INADEQUATE NCCN.

An important advantage of the NCOCA NCCN experiment, which is of great importance for uniformly labeled proteins, is

Table 1. $|\psi|$ Torsion Angles Measured in α-Spectrin SH3 Domain by INADEQUATE NCCN and NCOCA NCCN Experiments

	$\|\psi\|$ (deg)		ψ (deg)
residue	INADEQUATE NCCN	NCOCA NCCN	X-ray
L8	−	75 ± 20	149.6
		149 ± 16	
V9	−	158 ± 9	157.5
L12	−	<151	−21
D14	148 ± 12	−	145.5
Y15	<146	<150	117.8
P20		<147	−36.6
V23	158 ± 9	156 ± 10	164
T24	152 ± 8	154 ± 9	147.5
K27	<137	<141	130
G28	<146	<156	−9.3
I30	−	<144	114.5
T32	<141	<145	123.3
L34	−	<148	−42
S36	−	<146	28.8
T37	<145	<144	−33.7
K39	−	<145	−21.9
V44	162 ± 12	167 ± 13	170.9
Q50	−	74 ± 20	145.9
		148 ± 14	
G51	180 ± 11	180 ± 20	−175.7
F52	−	74 ± 24	145.2
		141 ± 16	
P54	<142	<151	129
A55	<145	−	−35.4
V58	154 ± 9	159 ± 6	153.7
K60	−	<156	130.7

that it provides significantly better spectral resolution. In addition, the NCOCA polarization transfer scheme can be extended to an NCOCACB experiment by using an additional selective mixing step[55] to transfer polarization from $^{13}C_{\alpha i}$ to $^{13}C_{\beta i}$ and $^{13}C_{\gamma i}$ prior to detection. The chemical shift dispersion of $^{13}C_{\beta i}$ and $^{13}C_{\gamma i}$ carbons is generally better than that of $^{13}C_{\alpha i}$, and one can expect an additional resolution enhancement. Therefore, in small peptides, or in other cases when sufficient spectral resolution can be achieved in the DQ-SQ $^{13}C-^{13}C$-correlation spectrum, it is advisable to use the INADEQUATE NCCN experiment. In larger systems the NCOCA NCCN scheme seems to be more suitable for constraining NCCN conformations.

Conclusions

In conclusion, we have demonstrated the feasibility of the measurement of multiple ψ-torsion angle constraints in a uniformly $^{13}C,^{15}N$ labeled protein. The combination of the chemical shift correlation and NCCN dipolar correlation experiment makes it a powerful tool for structural determinations in biological solids. Two experiments, INADEQUATE NCCN and NCOCA NCCN are applied to a uniformly $^{13}C,^{15}N$-labeled α-spectrin SH3 domain. While the INADEQUATE NCCN experiment provides better signal-to-noise and is better compensated with respect to the homonuclear *J*-coupling effects, the NCOCA NCCN scheme has the advantage of having better spectral resolution, which results in the larger number of ψ torsion angle constraints that can be determined. The sensitivity of the experiment is optimal for the conformations with $|\psi| > 145°$.

We expect that the NCCN and similar dipolar correlation methods will become an integral component of structural studies

(55) Verel, R.; Ernst, M.; Meier, B. H. *J. Magn. Reson.* **2001**, *150*, 81−99.

in uniformly labeled proteins. These methods are able to provide direct experimental restraints on the local backbone conformations. The combination of dipolar-[38] or chemical shift-based[56−58] torsion angle methods and of internuclear distance measurement techniques[19,29] will make it possible to obtain reliable solid-state NMR 3D protein structures.

Acknowledgment. We thank Nathan Astrof and Mike McMahon for stimulating discussions. C.P.J. thanks the NSF for a Predoctoral Fellowship. This research was supported by NIH Grants GM-23403 and RR-00995.

JA029082C

(56) Spera, S.; Bax, A. *J. Am. Chem. Soc.* **1991**, *113*, 5490−5492.
(57) Cornilescu, G.; Delaglio, F.; Bax, A. *J. Biomol. NMR* **1999**, *13*, 289−302.
(58) Luca, S.; Filippov, D. V.; van Boom, J. H.; Oschkinat, H.; de Groot, H. J. M.; Baldus, M. *J. Biomol. NMR* **2001**, *20*, 325−331.